The delayed rise of present-day mammals — Supplementary Information

Table of contents

Supplementary methods 3

Supertree construction 3

Establishing times of divergence 7

Fossil calibration points 7

Relative molecular dates 8

Interpolating missing dates and correcting negative branch lengths 13

Temporal pattern of diversification 14

Rates through time 15

Genera-through-time plots 16

Supplementary results 17

Divergence dates in the mammalian supertree 17

Results of sensitivity analyses 18

Consistency among major groups 18

Supplementary references 19

Supplementary figures 23

Supplementary figure 1 (see file Bininda_SupplData1.txt) 23

Supplementary figure 2 24

Supplementary figure 3 25

Supplementary figure 4 26

Supplementary tables 27

Supplementary table 1 27

Supplementary table 2 (see file Bininda_SupplData2.xls) 29

Supplementary table 3 30

Supplementary table 4 32

Supplementary table 5 (see file Bininda_SupplData3.xls) 35

Additional files (Supplementary data)

Bininda_SupplData1.txt

Bininda_SupplData2.xls

Bininda_SupplData3.xls

Supplementary methods

Supertree construction. Supertree construction operates by combining the phylogenetic hypotheses specified by primary character data, rather than these data themselves. It thereby can include more of the known phylogenetic information by avoiding the requirement of conventional analyses that all the character data have to be analyzable using a single optimization criterion. Clearly, not all character data fulfil this requirement (e.g., molecular distance data versus molecular sequence data) and it is arguable whether a single optimization criterion exists that itself is optimal for the analysis of all different data types. A supertree approach instead allows a divide-and-conquer strategy in which each partition (e.g., gene tree or morphological data set) can be analyzed in the most robust and appropriate fashion possible, leading to source trees of the highest possible accuracy[22,43]. Simulation studies have repeatedly shown that a supertree approach based on good data shows equal performance to a direct analysis of these same data[44–47], indicating that the loss of information inherent in combining trees is not unduly detrimental. For these reasons, supertree construction is currently better able to yield comprehensive phylogenies of large groups such as extant Mammalia.

Even so, a global supertree analysis of the 4500+ extant species of Mammalia probably remains computationally infeasible at this time. We therefore employed a compartmentalized approach[48] in which the global supertree was constructed by combining hierarchically nested supertrees. The foundation for the supertree is the family-level placental mammal supertree of Beck *et al.*[49], on to which more detailed trees for the various major lineages (generally orders) were grafted (see Supplementary Table 1). Although this procedure does invoke the strong assumption of the monophyly of each of these lineages, these assumptions were based on the most recent and uncontroversial phylogenetic knowledge available. Furthermore, they were also tested via the Beck *et al.* supertree[49], which did not assume the monophyly of these lineages. The assumptions thus represent a reasonable trade-off to break a globally difficult problem into smaller, more manageable problems to potentially yield an end result with a higher global accuracy[50]. To complete the supertree for all mammals, we assumed that the

marsupials and monotremes formed successive sister groups to the placentals, in line with the overwhelming majority of recent studies[51–53].

Deeper portions of the supertree were obtained from the combination of newly derived supertrees with pre-existing ones for Carnivora, Chiroptera, "Insectivora", and Lagomorpha (see Supplementary Table 1). The insectivore supertree, however, was reapportioned into Afrosoricida and Eulipotyphla following the Beck *et al.* topology[49]. Furthermore, Crocidurinae, which were not considered in the insectivore supertree, were also added as the sister group to Sorcinae within Eulipotyphla, with each genus within the family comprising an unresolved polytomy. For lineages comprising two or fewer species according to Wilson and Reeder[23] (Aplodontidae, Dermoptera, Pedetidae, Proboscidea, and Tubulidentata), these species were simply substituted onto the supertree. For the three species in Monotremata, we assumed that the two echidna species (*Tachyglossus aculeatus* and *Zaglossus bruijni*) were more closely related to each other than either is to the platypus (*Ornithorhynchus anatinus*) following Flannery *et al.*[54]. In all but one case (Rodentia; see below), the intra-lineage relationships in the individual studies, which were generally supported by more data, were preferred to those in the Beck *et al.*[49] supertree. Specifically, Supplementary Table 1 provides a list of all clades in the Beck *et al.* supertree that were replaced with new or previously published supertrees.

A standard methodology was applied in the construction of all new supertrees to ensure consistency. Source trees were gleaned from the literature according to an explicit source tree collection protocol[29] to minimize both data duplication (e.g., where the same data set underlies more than one source tree) and the inclusion of source trees of lesser quality (e.g., taxonomies or those based on appeals to authority)[55]. As demonstrated by Beck *et al.*[49] based on a case study of the Liu *et al.*[56] supertree, the protocol indeed proved highly effective in meeting these goals. Furthermore, all species names in the source trees were standardized to those found in Wilson and Reeder[23] using the Perl script synonoTree v2.x[29]. Only extant species were included in the final tree; species recognized by Wilson and Reeder[23] but

considered extinct in the 2004 IUCN Red List (http://www.redlist.org/) were excluded from the supertree, usually by pruning them at the level of the source trees before the supertree analysis (following ref. 57). Otherwise, extinct species were pruned from the existing supertrees, including those for the Cetartiodactyla and Marsupialia.

Although an update to Wilson and Reeder[23] has been published recently[58], it was unavailable during the tree construction process. The update contains 260 species discovered *de novo* since the previous version was published, an increase of 5.7%; all other changes stem from either taxonomic revision (e.g., elevation of a subspecies to full species status) or a possibly improved listing of recently extinct forms. Given that the latter group of species would be excluded in our analyses and that species from the former will generally diverge from their sister species very close to the present, their exclusion will not affect our main results concerning the timing of mammalian diversification before 25 million years (Myr) ago to any substantial degree if at all.

All supertrees were constructed using standard, unweighted matrix representation with parsimony (MRP[30,31]), where the topologies of the source trees were converted into a partial binary matrix: species descended from a given node were coded as 1; those that were not, but were present on the tree were coded as 0; and all other taxa were coded as ? for that source tree. Except for the Beck *et al.*[49], Muridae, Perissodactyla, and Primates supertrees, a hypothetical all-zero outgroup was added to each matrix consisting of the concatenated matrix representations of the source trees; the former four analyses instead used a semi-rooted form of MRP[59], where only robustly rooted source trees were rooted with an all-zero outgroup; otherwise, the outgroup received '?'. All matrices were analyzed using a parsimony criterion with the search strategy being tailored to the size of the matrix. For the larger groups, we used the parsimony ratchet[60] to facilitate a more efficient search of tree space. Where appropriate, we also used safe taxonomic reduction[61] as implemented in the Perl script PerlEQ v1.0.x (Jeffries and Wilkinson, unpubl.) to identify poorly known species that would contribute to substantial loss of local resolution. We used the results of this

analysis as a guide for pruning potentially problematic species from the source trees before subsequent recoding and re-analysis of the MRP matrices (following ref. 62) to improve resolution. In all cases, the final tree for each group was a strict consensus of all equally most parsimonious trees. Additional detail on individual search strategies can be found in the respective publications.

Two groups, Rodentia and Primates, warrant special mention. Both the large size of Rodentia (~2000 extant species) together with the extreme paucity and/or highly conflicting nature of information present for many subgroups presented particular problems. As such, the family-level structure within Rodentia is based on the Beck *et al.* supertree[49]. Apart from the suborder Hystricognathi, the superfamily Geomyoidea, and the families Dipodidae, Muridae, Myoxidae, and Sciuridae, for which new supertrees were constructed, additional structure within families was derived from the taxonomies of Wilson and Reeder[23] and McKenna and Bell[63]. The murid supertree in particular was derived from the two taxonomies in combination with 44 novel gene trees. The gene trees were derived from phylogenetic analyses of the same data sets as used to date the supertree subsequently (see below). Phylogenetic analyses used PHYML v2.4.4[64] under the appropriate model of evolution as determined using ModelTEST v3.6[65]. However, because of the large number of murid species and lack of information for most of them, the terminal taxa on all murid source trees including the taxonomies were synonymised to the genus level using synonoTree. A genus-level supertree was therefore obtained, with the monophyly of the major subfamilies Avicolinae, Cricetinae, Dendromurinae, Gerbillinae, Murinae, Nesomyinae, and Sigmodontinae being specified with respect to one another using a backbone constraint tree in PAUP*. The final species-level supertree for murids was derived by substituting all species on to the genus-level supertree, generally as unresolved polytomies (except where clear within-genus structure was present in Musser and Carleton[66]). As a result, the murid portion of the supertree is comparatively poorly resolved, particularly close to the tips.

Because existing supertrees of the primates[34,67] do not reflect the great deal of work on primate phylogeny that has since occurred, our primate phylogeny derives from a combination of the Purvis[34] source trees with a subsequent set compiled by Vos and Mooers[68] for their recent update to the primate supertree. As far as possible, both data sets were corrected for source-tree non-independence according to the protocol of Bininda-Emonds *et al.*[29].

Establishing times of divergence. Following Purvis[34], Bininda-Emonds *et al.*[69], and Jones *et al.*[36], divergence times for all nodes on the supertree were estimated by a combination of fossil and/or molecular dates under the assumption of a local molecular clock[34] or, when such estimates were unavailable, from dates interpolated from other robustly dated nodes using a pure birth model.

Fossil calibration points

The use of fossil data to derive date estimates presents several inherent problems. First, fossils are often used to calibrate date estimates among extant taxa only (as it this case here), requiring some robust method to associate a given fossil to a crown group clade. Second, the incomplete nature of the fossil record means that fossils invariably provide underestimates of the divergence times[33]; the underestimates are expected to be increasingly severe with the decreasing quality of the fossil record. Third, the date assigned to a given fossil often corresponds to a chronostratigraphic interval and thus really represents a range and not a point (chronometric) estimate.

Because of the crucial impact of fossil calibration points on the accuracy of molecular date estimates[69,70], we have attempted to be as conservative as possible regarding the above problems. Thus, we targeted only major lineages within mammals (generally orders), which because of the nested structure of the taxonomic hierarchy are more likely to have fossil information associated with them than are the lower hierarchical levels. Also, to be associated with a given node, a fossil species must have been demonstrated to share at least one

synapomorphy of that clade in a robust cladistic analysis. We then held the fossil to represent the divergence time between the lowest extant taxonomic level to which it was assigned (usually a family) and the sister taxon of it (= stem-group node of Renner[70]). Finally, where a fossil date was represented by a range, we used the midpoint of the range as the point estimate. All 30 fossils used here were taken to represent minimum ages for the nodes that they were assigned to (see Supplementary Table 3).

Relative molecular dates

Molecular date estimates were obtained by fitting sequence data to the topology of the supertree (following ref. 36) and using a local molecular clock in which the age of a node was held to be some percentage of the age of a node ancestral to it based on the relative branch lengths[34]. Except for the murid portion of the supertree, all gene sequences used were independent of the supertree topology insofar as they contributed to only a fraction of the over 2600 source trees used (see Supplementary Table 1).

Mammalian sequence data were mined from the 534 225 entries in the primate, rodent, and mammal sections of GenBank release 144 (October 15, 2004) using the Perl script GenBankStrip v2.0 to identify the genes in each accession according to the annotated details provided. This procedure is highly dependent on the accuracy of the annotations given and only has limited facilities for dealing with gene synonyms or typographical errors. However, unlike procedures designed to mine genetic data based on sequence similarity (e.g., blastclust, part of the BLAST package[71]), GenBankStrip is better able to mine complete sequences over a broader taxonomic range and, given an accurate annotation, can separate paralogs from orthologs and exclude pseudogenes. It also does not incur the same memory requirements (e.g., blastclust has an upper limit on the order of 250 000 sequences; Michael J. Sanderson, pers. comm.). Using GenBankStrip, all genes were identified and the corresponding sequences saved to individual fasta-formatted files for each gene. Thereafter, the gene data were post-processed such that only genes sampled for more than 50 species (according to the NCBI taxonomy;

http://www.ncbi.nlm.nih.gov/entrez/query.fcgi?db=Taxonomy) were retained and then only sequences of the 10 longest lengths for each gene, where these lengths had to be greater than either 50 (tRNAs) or 200 bp (all other genes). This resulted in an initial data set of 58 382 sequences distributed among 3179 NCBI species and 66 genes (32 nDNA, 19 tRNA, and 15 other mtDNA).

The sequences for each gene were then aligned using any of MUSCLE[72] for the tRNA genes, ClustalW[73] for other non-coding genes or genes with UTRs, or transAlign[74] with ClustalW for genes consisting entirely of coding DNA. The initial alignments were then examined by eye using Se-Al (http://evolve.zoo.ox.ac.uk/software.html?name=Se-Al) for outlier sequences disrupting the alignment. Such outliers were either corrected (e.g., if they were in the wrong orientation) or deleted and the sequences were re-aligned. A slightly different procedure was followed for the three largest data sets: *MT-CYB* (9814 sequences), *MT-RNR1* (1255 sequences), and *MT-RNR2* (1278 sequences). For the former, the sequences were split into four equally-sized partitions (2453 or 2454 sequences each) alphabetically by species name. Each partition was then aligned separately using transAlign with ClustalW and subsequently merged by hand using Se-Al. For each of the two rRNA genes, the initial alignments were 'cleaned' (see below) and the resulting data sets were profiled aligned to a representative set of Carnivora sequences that had been independently aligned by eye against a structural model for mammals for other purposes; the latter reference sequences were then pruned from the data set.

All alignments were then examined manually and improved as needed (including paring the ends of isolated sequences that did not overlap with the vast majority of the remaining sequences). At this point, it was noted that each of the *LCAT* and *C-MYC* alignments consisted of two non-overlapping blocks of distinct regions of the gene that were bridged by a limited number of more complete sequences. Each alignment was thus divided into two separate alignments corresponding to each block. It was also noticed that the

alignments for the nuclear genes *TNF* and *TTR* did not contain sufficient information to justify their further analysis.

Each data set was then 'cleaned' using the Perl script seqCleaner v1.0.2 to remove any sequences with greater than 5% ambiguous nucleotides (i.e., Ns), to standardize the species names according to the taxonomy presented in Wilson and Reeder[23], to ensure that all sequences overlapped pairwise by 25 or 100 bps (for tRNAs and all other genes, respectively), and to retain five representative sequences for those species that were sampled more often than this. The five sequences retained were 1) the one closest to the consensus sequence of all specimens for that species, 2) the two furthest from the consensus sequence, and 3) two that were intermediate between these extremes. In all cases, similarity was judged according to a Jukes-Cantor[75] model with the lengths of the sequences being taken into account to attempt to retain the longest sequences. For the three largest data sets—*MT-CYB*, *MT-RNR1* and *MT-RNR2*—only a single specimen per species (that closest to the consensus sequence) was retained to facilitate subsequent analyses and/or further aligning. The final data set consisted of 51 089 bp from 66 genes (32 nDNA, 19 tRNA, and 15 other mtDNA), with the two nuclear genes *LCAT* and *C-MYC* each being represented by two independent parts. A total of 2182 different mammalian species were variously represented across the individual alignments.

Representative outgroup sequences from the chicken (*Gallus gallus*) and/or either of the African or western clawed frogs (*Xenopus laevis* and *Xenopus tropicalis*, respectively) were then added to each data set. Finally, each individual data set was fitted to the supertree topology under a maximum likelihood (ML) framework to determine the branch lengths. In so doing, taxa not present in the data set were pruned from the supertree and individual species represented by multiple specimens were replaced in the supertree by a new unresolved clade from which all the specimens were descended. The appropriate model of evolution for each data set was determined using the AIC criterion in ModelTEST, with the tree used in these analyses being the modified mammal supertree instead of the usual NJ tree

(see Supplementary Table 4). Additionally, all genes were tested as to whether they satisfied a molecular clock using a likelihood-ratio test. Only *MT-TI*, *MT-TM*, *SRY*, and *TSPY* were found to do so at a nominal alpha level of 0.05 corrected for multiple comparisons using the sequential Bonferroni method of Rice[76]. ML branch lengths were then determined using PAUP* v4.0b10[32]. Polytomies in the supertree were not resolved during the process because of the requirement to calculate branch lengths relative to only those nodes present on the supertree. The relative branch lengths for each gene tree relative to the topology of the supertree were calculated using the Perl script relDate v2.3, which implements Purvis'[34] local-clock model that essentially smoothes substitution rates across sister groups. Only the gene trees for the clock-like genes *MT-TI*, *MT-TM*, *SRY*, and *TSPY* were considered to be rooted, thereby providing relative branch length that included the root node.

Divergence dates in the supertree were then determined by calibrating the relative molecular branch lengths (taken relative to an ancestral node only) using the fossil dates. For each node, the estimated divergence date was taken to be the oldest value from either 1) the oldest fossil date or 2) the median of up to 68 relative molecular dates and/or the oldest fossil date, thereby recognizing that the fossil dates represent minimum age constraints on a given node. The recursive nature of the procedure (whereby a relative date is based on the date of an ancestral node, which in turn can be based on other fossil information and/or the relative dates from the same or other genes) means that multiple, local calibrations are being made. Even so, the procedure does rely heavily on more basal date estimates and that for the mammalian root (i.e., the divergence between monotremes and the therian mammals) in particular. This latter value was estimated to be 166.2 Myr ago based on the acceptance of the enigmatic Middle Jurassic (Bathonian) Malagasy fossil *Ambondro mahabo*[35], the known remains of which comprise only three lower teeth in a jaw fragment, as a probable crown-group mammal, given that it has been associated with either monotremes[51,77,78] or placental mammals[79] in robust cladistic analyses.

Even so, the use of *A. mahabo* to estimate the date of the root node of the supertree undoubtedly yields a severe underestimate of the true value. For instance, it is possible to use the oft-cited value of 310 Myr ago for the bird-mammal split[80] as the ultimate calibration point (although we did not do so owing to the lack of any supporting fossil evidence meeting our criteria above; the date has also come recently under severe criticism[81]); doing so would yield a date estimate for the mammal root of 189.0 Myr ago, an increase of 13.7%. Moreover, unless one argues that the limited fossil record for holotherian mammals in the later Jurassic and Early Cretaceous is representative in a truly statistical sense, it cannot be simply asserted that "each new discovery [like *Ambondro*] reduces the already slim likelihood that the non-occurrence of therians before ~110 Myr ago is due to a preservational / sampling effect"[35:59–60]. For instance, at ~124 Myr ago, the stem therians *Eomaia* and *Sinodelphys* are each 13% older than the earlier supposed basal Albian initiation of their clades—a significant amount.

Compared to other recently developed methods of estimating divergence times (for recent reviews, see refs 70,82), our ML-based dating method still employs the concept of rate smoothing (across sister taxa), but is computationally far less intensive. The latter is a key consideration given the size of the problem. For instance, both non-parametric rate smoothing (NPRS[83]) and penalized likelihood (PL[84]) are unlikely to be able to estimate divergence times for a tree of this size, or even for some of the larger gene trees (Michael J. Sanderson, pers. comm.), and it seems reasonable that this would apply to the remaining Bayesian methods as well. Moreover, the divide-and-conquer nature of the method, whereby each gene is analyzed individually, readily allows the use of different models of evolution that are optimally tailored for each gene. Although the use of mixed models in a simultaneous analysis is possible in a ML / Bayesian context, the accuracy of doing so, at least for phylogenetic inference, has recently been called into question by Mossel and Vigoda[85], who instead argue in favour of a divide-and-conquer approach in such cases. Additionally, our procedure also avoids potential problems deriving from missing data. The latter issue is particularly relevant here because the highly unequal taxonomic coverage among the data sets, which range in size from 33 to 1284 sequences (one of the *LCAT* data sets and *MT-CYB*, respectively), would

result in an extremely high proportion of missing data (91.1%) in a single, concatenated data set.

Interpolating missing dates and correcting negative branch lengths

Using the methodology described, date estimates were obtained for 1322 of the 2108 nodes (= 62.7%) in the supertree, together with 95% confidence intervals as obtained from the variation among the date estimates from the individual genes for that node. Dates for the remaining 786 nodes were interpolated from these estimates according to the pure birth model in Purvis[34] as implemented in the Perl script chronoGrapher v1.3.3. In this model, the interpolated age of a node is determined as the age of a reference node scaled by the natural logarithm of the ratio of the species richness of both clades. This formula has been criticized in that it does not truly correspond to a pure birth model[68]. When the procedure is applied iteratively (i.e., an interpolated date is derived from an interpolated date), the rate of cladogenesis slows down instead of increasing as it should under a pure birth model[68]. However, this effect does not occur for fully balanced trees (unpubl. data) and only becomes noticeable when applied iteratively (i.e., when a date is interpolated from another interpolated date). As implemented in chronoGrapher, interpolated dates are based on the average of up to five immediately ancestral, robustly dated nodes (inversely weighted according to node depth) and any robustly dated direct daughter nodes, which should altogether minimize any attendant errors. Furthermore, none of the analyses reported in the paper are based on any interpolated dates.

Negative branch lengths in the supertree were corrected using chronoGrapher. For a given negative branch, the parent and daughter node each received the average of their ages corrected by a factor of +0.1 or –0.1 Myr, respectively, to maintain the topological information in the supertree. Because this single correction could either fail to correct other negative branch lengths or even generate new ones, the process was performed iteratively until no further negative branch lengths were obtained. The 30 fossil calibration points also served as minimal age constraints to be respected during the correction process. Repeating

this entire procedure with the upper and lower 95% confidence intervals of the relative molecular dates, yielded corresponding confidence intervals for all date estimates on the supertree, including those interpolated using the pure birth model.

An electronic version of the dated supertree (Supplementary Fig. 1) is also available from any authors on request. In addition, all Perl scripts are freely available from http://www.uni-oldenburg.de/molekularesystematik/33997.html and the aligned sequence data are available on request from the first author.

Temporal pattern of diversification. Phylogenies of extant species can in principle provide information about the instantaneous rates of speciation (λ) and extinction (μ). Our primary interest here is in temporal patterns in the net rate of diversification, r ($= \lambda - \mu$). Inference about the recent past is hampered because an increase in r cannot be distinguished from a process in which λ and μ are constant[86]. However, divergences older than about $1 / (\lambda - \mu)$ (ref. 19) are informative about whether and how r changed over time. The deep branching structure of our tree is well resolved. We restrict our analyses to the part of mammalian history for which the tree is at least 85% resolved and for which no dates were interpolated to minimize biases caused by 'soft' polytomies or interpolation. This portion of the overall tree covers the first 82 lineages, from 166.2 to 48.2 Myr ago; for placentals and marsupials, the corresponding figures are 70 lineages (98.5 to 48.2 Myr ago) and 20 lineages (82.5 to 34.9 Myr ago), respectively. If r was constant, a plot of the logarithm of lineage number against time is expected to yield a straight line, the slope of which estimates r (refs 18,19). To test whether r changed over time, we used two-tailed γ tests[20]. The γ statistic comes from a standard normal distribution if r has been constant, so values outside the range ± 1.96 indicate a significant trend in r. Moreover, a significantly positive γ so far back in the past would not be consistent with a constant-rates birth-death process.

The γ test does not distinguish whether any changes in diversification rate were gradual or sudden, requiring another approach to distinguish between these scenarios. Under a constant-rate pure-birth process, the product of lineage number (n) and waiting time to the

next speciation (t_n) has a constant expectation[87] and an exponential distribution[86], although zeroes are introduced by both polytomies and limited precision of dates; $\ln(n.t_n + 1)$ is roughly normally distributed, so we use this as our response variable (y). If diversification rate changed gradually and consistently, y should show a temporal trend, whereas a sudden change should cause a step-like alteration. We therefore model y as a function of geological time using both linear regression and a one-step regression tree that finds the geological age that splits y into two groups with lowest residual deviance). AIC_c[88] is used to assess which of these models provides the better description of the data, and to compute their evidence weights.

Rates through time. The above approach is reliable only for well-resolved phylogenies where the branching dates are estimated directly from data. The mammal phylogeny is increasingly unresolved after about 50 Myr ago, with an increasing proportion of node dates being interpolated, such that a different approach is needed to obtain reliable inferences about dynamics after this time. We therefore analysed the set of branches for which the start and end dates are estimated directly from data, and which do not start at a polytomy. There are 1733 such branches, 940 of which end in a speciation event and 793 in a present-day species. However, estimates of net diversification rate are still subject to upward bias for times more recent than $1 / (\lambda - \mu)$ (ref. 19), and the most recent rate estimates will be biased downward by lack of resolution within more diverse genera and by any reluctance to name the products of recent splits as separate species. We therefore do not interpret changes in the rates over the last 25 Myr. Average diversification rates were estimated by survival analyses within each geological age (pre-Pleistocene) or sub-epoch (Pleistocene) in the timescale of Gradstein *et al*.[89] using generalised linear models (GLMs) with Poisson errors[37]. The same approach was used to test for a significant rate differences between the latest Cretaceous (Maastrichtian) and earliest Tertiary (Danian) ages. Diversification rate was also modelled as a continuous function of time using generalized additive models (GAMs)[38]. GAMs were used because the form and degree of complexity of any relationship between r and time could not be predicted *a priori*. For each 0.1 Myr interval (the limit of precision of node ages in the phylogeny), we

scored the number of lineages present that did and did not speciate at the end of the interval. We constructed a binomial response variable from these data, and modelled it as a smooth function of time, rescaling the fitted values to convert them into rates per lineage per Myr. Because the relationship could in principle be very complex, the basis dimension (k) for the fitted curves (Fig. 2b in main text, Supplementary Figs 2 and 3) was set high enough to permit a knot every 1 Myr. Unbiased risk estimation (UBRE) was then used to estimate smoothing parameters and the effective degrees of freedom for the smooth term. To avoid overfitting, the gamma parameter was set to 1.4 (increasing the penalty for complexity in the smooth term) as recommended by Wood[38]. Hypothesis-testing was based on unpenalized GAMs[38]; for these, k was set to 10 because statistical power falls as k is increased. Nested models (time-dependent versus constant r) were compared using ANOVA using χ^2 tests.

Genera-through-time plots. We gathered data on the occurrence of mammalian genera in 11 geological intervals (sub- epochs) from Late Triassic (228–199.6Ma) until Late Eocene (37.2–33.9Ma) using the Unitaxon database. The source file used as the basis for these analyses was the McKenna and Bell-based[42] Mammalia.3/06.txn (available from ftp://ftp.amnh.org/pub/people/mckenna/), which was run on The Unitaxon Classification Browser software, v2.0, available from Mathemaesthetics, Inc., Boulder, Colorado (www.mathemaesthetics.com). The 1804 genera in this database (see Supplementary Table 5), some of which fall outside the clades Theria and Monotremata, were assigned to sub-epoch intervals on the basis of a positive occurrence record or interpolation if the taxon was recorded either side of a particular interval. Time in millions of years of the geological periods followed the International Geological Time Scale[89]. We assigned genera into one of two groups: (1) genera whose family diversity was exclusively or predominantly Paleocene or older (≥55.8Ma) and (2) genera whose family diversity was exclusively or predominantly Eocene or younger (<55.8Ma). This procedure allowed separation of family-level taxa into those that started to diversify before the Eocene from those that diversified after. If equal numbers of genera were present on either side of the split within a given family, the family as

a whole was assigned to group 1. If no assignment of a genus to family was available (i.e., genus was *incertae sedis* as to family) the group assignment was based on individual age.

Supplementary results

Divergence dates in the mammalian supertree. Roughly 63% of the nodes (1322 of 2108) were dated based on one or more molecular and/or fossil estimates (Supplementary Table 2). The average number of such estimates for these nodes was 6.4, with the maximum being 63 (the node corresponding to Euarchontoglires). Except for the root of the tree, all the basal-most nodes, and all but two nodes (nodes 1410 and 1449; both within Chiroptera) inferred to be older than the K-T boundary, are based on at least 16 molecular and/or fossil estimates. Confidence intervals for the date estimates, as estimated by the standard error, are ±1.9 million years (Myr) on average, with an average coefficient of variation of 35.2%. For seven nodes, the median of the molecular and fossil dates underestimated that of the fossil information alone: Monotremata (by 10.0 Myr or 15.7%), Cetacea (by 22.9 Myr or 43.8%), Eulipotyphla (by 2.4 Myr or 3.0%) Sirenia (by 17.0 Myr or 32.6%), Proboscidea (by 13.6 Myr or 70.0%), Marsupialia (by 17.6 Myr or 21.3%), and Diprotodontia + *Dromciops gliroides* (by 3.9 Myr or 6.1%).

Our divergence date estimates correlate significantly with those of Springer *et al.*[8] for the 37 nodes in common to both trees (correlation coefficient for ln-transformed dates = 0.951; $Z = 10.742$; $P < 0.0001$). They are, however, significantly older (mean difference of ln-transformed values = 0.119 (or 13.7%), paired $t = 5.466$, $df = 36$, two-tailed $P < 0.0001$), and the difference would be even greater had our dates been calibrated on the chicken-mammal split (results not shown). By contrast, the respective confidence intervals in the date estimate for a given node are not correlated between the two studies (correlation coefficient for ln-transformed dates = 0.228; $Z = 1.353$; $P = 0.1761$), with the credibility intervals in Springer *et al.*[8] being significantly larger (mean difference of ln-transformed values = 0.439 (or 21.4%), paired $t = 4.440$, $df = 36$, two-tailed $P < 0.0001$).

Results of sensitivity analyses. The supertree based on the upper and lower 95% confidence interval dates showed a slightly different number of lineages surviving the K-T boundary from the 45 (40 placental, four marsupial, and one monotreme) obtained using the inferred dates. For the upper dates, a total of 58 lineages crossed the boundary (49 placental, seven marsupial, and three monotreme), whereas only 44 did so (40 placental, three marsupial, and one monotreme) for the lower dates.

Analyses using the upper and lower 95% confidence interval dates parallel those for the inferred dates (Supplementary Figs 2 and 3, and Fig. 2 in main text, respectively). Analysis of rates through time indicates highly significant variation (upper dates: $\chi^2_9 = 29.1$, $P = 0.0006$; lower dates: $\chi^2_9 = 35.41$, $P << 0.001$). The peaks in the estimated rates (smooth lines in Supplementary Figs 2b and 3b) are at 91.1 and 87.1 Myr ago for the upper and lower confidence intervals dates, respectively. Neither set of dates shows a significant rate difference between the latest Cretaceous (Maastrichtian) and earliest Tertiary (Danian) (upper dates: $z = –0.104$, $df = 106$, $P = 0.92$; lower dates: $z = –1.773$, $df = 90$, $P = 0.08$). The upper dates favour a step-change slowdown in placental rates over a smooth change, with the rate decreasing at 84.8 Myr ago (evidence weight = 94.9%), whereas the lower dates very slightly favour a smooth decrease in the net rate of placental diversification (evidence weight = 61.3%).

Consistency among major groups. Supplementary Fig. 4 shows estimated diversification rates through time for four major groups, Euarchontoglires, Laurasiatheria, Xenarthra/Afrotheria (grouped together because of small individual sample sizes) and Marsupialia. Temporal patterns are broadly similar among these crown groups. The first three originated in the period of highest overall rates (around 85–90 Myr ago). Marsupials show a slight rate peak around K-T, consistent with their small, but proportionately large, increase in lineage number around this time (from three to six in the period 65.8–63.6 Myr ago; also Fig. 2a in the main text). Xenarthra/Afrotheria consistently show the lowest rate of diversification, and their rate does not increase in the Eocene.

Supplementary references

43. Bininda-Emonds, O. R. P. The evolution of supertrees. *Trends in Ecology and Evolution* **19**, 315–322 (2004).
44. Bininda-Emonds, O. R. P. & Sanderson, M. J. Assessment of the accuracy of matrix representation with parsimony supertree construction. *Systematic Biology* **50**, 565–579 (2001).
45. Chen, D., Diao, L., Eulenstein, O., Fernández-Baca, D. & Sanderson, M. J. in *Bioconsensus* (eds. Janowitz, M. F., Lapointe, F.-J., McMorris, F. R., Mirkin, B. & Roberts, F. S.) 135–160 (American Mathematical Society, Providence, RI, 2003).
46. Levasseur, C. & Lapointe, F.-J. in *Bioconsensus* (eds. Janowitz, M. F., Lapointe, F.-J., McMorris, F. R., Mirkin, B. & Roberts, F. S.) 221–230 (American Mathematical Society, Providence, RI, 2003).
47. Piaggio-Talice, R., Burleigh, J. G. & Eulenstein, O. in *Phylogenetic supertrees: combining information to reveal the Tree of Life* (ed. Bininda-Emonds, O. R. P.) 173–191 (Kluwer Academic, Dordrecht, the Netherlands, 2004).
48. Mishler, B. D. Cladistic analysis of molecular and morphological data. *American Journal of Physical Anthropology* **94**, 143–156 (1994).
49. Beck, R. M. D., Bininda-Emonds, O. R. P., Cardillo, M., Liu, F.-G. R. & Purvis, A. A higher-level MRP supertree of placental mammals. *BMC Evolutionary Biology* **6** (2006).
50. Roshan, U., Moret, B. M. E., Williams, T. L. & Warnow, T. in *Phylogenetic supertrees: combining information to reveal the Tree of Life* (ed. Bininda-Emonds, O. R. P.) 301–328 (Kluwer Academic, Dordrecht, the Netherlands, 2004).
51. Luo, Z.-X., Kielan-Jaworowska, Z. & Cifelli, R. L. In quest for a phylogeny of Mesozoic mammals. *Acta Palaeontologica Polonica* **47**, 1–78 (2002).
52. van Rheede, T. *et al*. The platypus is its place: nuclear genes and indels confirm the sister group relation of monotremes and therians. *Molecular Biology and Evolution* **23**, 587–597 (2006).
53. Phillips, M. J. & Penny, D. The root of the mammalian tree inferred from whole mitochondrial genomes. *Molecular Phylogenetics and Evolution* **28**, 171–185 (2003).
54. Flannery, T. F., Archer, M., Rich, T. H. & Jones, R. A new family of monotremes from the Creatceous of Australia. *Nature* **377**, 418–420 (1995).
55. Gatesy, J., Matthee, C., DeSalle, R. & Hayashi, C. Resolution of a supertree/supermatrix paradox. *Systematic Biology* **51**, 652–664 (2002).
56. Liu, F.-G. R. *et al*. Molecular and morphological supertrees for eutherian (placental) mammals. *Science* **291**, 1786–1789 (2001).
57. Pisani, D., Yates, A. M., Langer, M. C. & Benton, M. J. A genus-level supertree of the Dinosauria. *Proceedings of the Royal Society of London B* **269**, 915–921 (2002).
58. Wilson, D. E. & Reeder, D. M. (eds.) *Mammal species of the world: a taxonomic and geographic reference* (John Hopkins University Press, Baltimore, 2005).
59. Bininda-Emonds, O. R. P., Beck, R. M. D. & Purvis, A. Getting to the roots of matrix representation. *Systematic Biology* **54**, 668–672 (2005).
60. Nixon, K. C. & Davis, J. I. Polymorphic taxa, missing values, and cladistic analysis. *Cladistics* **6**, 211–223 (1991).
61. Wilkinson, M. Common cladistic information and its consensus representation: reduced Adams and reduced cladistic consensus trees and profiles. *Systematic Biology* **43**, 343–368 (1994).

62. Pisani, D. & Wilkinson, M. Matrix representation with parsimony, taxonomic congruence, and total evidence. *Systematic Biology* **51**, 151–155 (2002).
63. McKenna, M. C. The alpha crystallin A chain of the eye lens and mammalian phylogeny. *Annales Zoologici Fennici* **28**, 349–360 (1991).
64. Guindon, S. & Gascuel, O. A simple, fast, and accurate algorithm to estimate large phylogenies by maximum likelihood. *Systematic Biology* **52**, 696–704 (2003).
65. Posada, D. & Crandall, K. A. MODELTEST: testing the model of DNA substitution. *Bioinformatics* **14**, 817–818 (1998).
66. Musser, G. G. & Carleton, M. D. in *Mammal species of the world: a taxonomic and geographic reference* (eds. Wilson, D. E. & Reeder, D. M.) 501–756 (Smithsonian Institution Press, Washington, 1993).
67. Purvis, A. & Webster, A. J. in *Comparative primate socioecology* (ed. Lee, P. C.) 44–70 (Cambridge University Press, Cambridge, 1999).
68. Vos, R. A. & Mooers, A. Ø. A dated MRP supertree for the order Primates. *Systematic Biology* (submitted).
69. Bininda-Emonds, O. R. P., Gittleman, J. L. & Purvis, A. Building large trees by combining phylogenetic information: a complete phylogeny of the extant Carnivora (Mammalia). *Biological Reviews* **74**, 143–175 (1999).
70. Renner, S. S. Relaxed molecular clocks for dating historical plant dispersal events. *Trends in Plant Science* **10**, 550–558 (2005).
71. Altschul, S. F., Gish, W., Miller, W., Myers, E. W. & Lipman, D. J. Basic local alignment search tool. *Journal of Molecular Biology* **215**, 403–410 (1990).
72. Edgar, R. C. MUSCLE: multiple sequence alignment with high accuracy and high throughput. *Nucleic Acids Research* **32**, 1792–1797 (2004).
73. Thompson, J. D., Higgins, D. G. & Gibson, T. J. CLUSTAL W: improving the sensitivity of progressive multiple sequence alignment through sequence weighting, position-specific gap penalties and weight matrix choice. *Nucleic Acids Research* **22**, 4673–4680 (1994).
74. Bininda-Emonds, O. R. P. transAlign: using amino acids to facilitate the multiple alignment of protein-coding DNA sequences. *BMC Bioinformatics* **6** (2005).
75. Jukes, T. H. & Cantor, C. R. in *Protein metabolism* (ed. Munro, M. N.) 21–132 (Academic Press, New York, 1969).
76. Rice, W. R. Analyzing tables of statistical tests. *Evolution* **43**, 223–225 (1989).
77. Luo, Z. X., Cifelli, R. L. & Kielan-Jaworowska, Z. Dual origin of tribosphenic mammals. *Nature* **409**, 53–57 (2001).
78. Luo, Z.-X., Crompton, A. W. & Sun, A.-L. A new mammaliform from the early Jurassic and evolution of mammalian characteristics. *Science* **292**, 1535–1540 (2001).
79. Woodburne, M. O., Rich, T. H. & Springer, M. S. The evolution of tribospheny and the antiquity of mammalian clades. *Molecular Phylogenetics and Evolution* **28**, 360–385 (2003).
80. Hedges, S. B. The origin and evolution of model organisms. *Nature Reviews Genetics* **3**, 838–849 (2002).
81. Graur, D. & Martin, W. Reading the entrails of chickens: molecular timescales of evolution and the illusion of precision. *Trends in Genetics* **20**, 80–86 (2004).
82. Welch, J. J. & Bromham, L. Molecular dating when rates vary. *Trends in Ecology and Evolution* **20**, 320–327 (2005).
83. Sanderson, M. J. A nonparametric approach to estimating divergence times in the absence of rate constancy. *Molecular Biology and Evolution* **14**, 1218–1231 (1997).

84. Sanderson, M. J. Estimating absolute rates of molecular evolution and divergence times: a penalized likelihood approach. *Molecular Biology and Evolution* **19**, 101–109 (2002).
85. Mossel, E. & Vigoda, E. Phylogenetic MCMC algorithms are misleading on mixtures of trees. *Science* **309**, 2207–2209 (2005).
86. Nee, S. Inferring speciation rates from phylogenies. *Evolution* **55**, 661–668 (2001).
87. Purvis, A., Nee, S. & Harvey, P. H. Macroevolutionary inferences from primate phylogeny. *Proceedings of the Royal Society of London B* **260**, 329–333 (1995).
88. Burnham, K. P. & Anderson, D. R. Multimodel inference - understanding AIC and BIC model selection. *Sociological Methods and Research* **33**, 261–304 (2004).
89. Gradstein, F. M., Ogg, J. G. & Smith, A. G. (eds.) *A geologic time scale 2004* (Cambridge University Press, Cambridge, 2004).
90. Grenyer, R. & Purvis, A. A composite species-level phylogeny of the 'Insectivora' (Mammalia: Order Lipotyphla Haeckel, 1866). *Journal of Zoology* **260**, 245–257 (2003).
91. Price, S. A., Bininda-Emonds, O. R. & Gittleman, J. L. A complete phylogeny of the whales, dolphins and even-toed hoofed mammals (Cetartiodactyla). *Biological Reviews* **80**, 445–473 (2005).
92. Jones, K. E., Purvis, A., MacLarnon, A., Bininda-Emonds, O. R. P. & Simmons, N. B. A phylogenetic supertree of the bats (Mammalia: Chiroptera). *Biological Reviews* **77**, 223–259 (2002).
93. Stoner, C. J., Bininda-Emonds, O. R. P. & Caro, T. M. The adaptive significance of coloration in lagomorphs. *Biological Journal of the Linnean Society* **79**, 309–328 (2003).
94. Cardillo, M., Bininda-Emonds, O. R. P., Boakes, E. & Purvis, A. A species-level phylogenetic supertree of marsupials. *Journal of Zoology* **264**, 11–31 (2005).
95. Pascual, R. *et al*. First discovery of monotremes in South America. *Nature* **356**, 704–705 (1992).
96. Ji, Q. *et al*. The earliest known eutherian mammal. *Nature* **416**, 816–822 (2002).
97. Meng, J., Wyss, A. R., Dawson, M. R. & Zhai, R. Primitive fossil rodent from Inner Mongolia and its implications for mammalian phylogeny. *Nature* **370**, 134–136 (1994).
98. Tong, Y. Fossil tree shrews from the Eocene Hetaoyuan formation of Xichuan, Henan. *Vertebrata Palasiatica* **26**, 214–220 (1988).
99. Ducrocq, S. *et al*. First fossil flying lemur: a dermopteran from the Late Eocene of Thailand. *Palaeontology (Oxford)* **35**, 373–380 (1992).
100. Beard, K. C., Qi, T., Dawson, M. R., Wang, B. & Li, C. A diverse new primate fauna from middle Eocene fissure-fillings in southeastern China. *Nature* **368**, 604–609 (1994).
101. Theodor, J. M., Rose, K. D. & Erfurt, J. in *The rise of placental mammals: origins and relationships of the major extant clades* (eds. Rose, K. D. & Archibald, J. D.) 215–233 (John Hopkins Press, Baltimore, 2005).
102. Gingerich, P. & Russell, D. *Pakicetus inachus*, a new archaeocete (Mammalia, Cetacea) from the Early-Middle Eocene Kuldana Formation of Kohat (Pakistan). *Contributions from the Museum of Paleontology University of Michigan* **25**, 235–246 (1981).
103. Rose, K. D., Emry, R. J., Gaudin, T. J. & Storch, G. in *The rise of placental mammals: origins and relationships of the major extant clades* (eds. Rose, K. D. & Archibald, J. D.) 106–126 (John Hopkins Press, Baltimore, 2005).

104. Storch, G. *Eomanis waldi*, ein Schuppentier aus dem Mittel-Eozän der "Grube Messel" bei Darmstadt (Mammalia: Pholidota). *Senckenbergiana Lethaea* **59**, 503–529 (1978).
105. Wyss, A. R. & Flynn, J. J. in *Mammalian phylogeny: placentals* (eds. Szalay, F. S., Novacek, M. J. & McKenna, M. C.) 32–52 (Springer-Verlag, New York, 1993).
106. Hunt, R. M., Jr. & Tedford, R. H. in *Mammalian phylogeny: placentals* (eds. Szalay, F. S., Novacek, M. J. & McKenna, M. C.) 53–73 (Springer-Verlag, New York, 1993).
107. Simmons, N. B. in *The rise of placental mammals: origins and relationships of the major extant clades* (eds. Rose, K. D. & Archibald, J. D.) 159–174 (John Hopkins Press, Baltimore, 2005).
108. MacPhee, R. D. E. Morphology, adaptations, and relationships of *Plesiorycteropus*, and a diagnosis of a new order of eutherian mammals. *Bulletin of the American Museum of Natural History* **220**, 1–214 (1994).
109. MacPhee, R. D. E. & Novacek, M. J. in *Mammalian phylogeny: placentals* (eds. Szalay, F. S., Novacek, M. J. & McKenna, M. C.) 13–31 (Springer-Verlag, New York, 1993).
110. Tassy, P. *et al*. A new *Stegalophodon* (Proboscidea, Mammalia) from the early Miocene of northern Thailand. *Géobios* **25**, 511–523 (1992).
111. Case, J. A., Goin, F. J. & Woodburne, M. O. "South American" marsupials from the Late Cretaceous of North America and the origin of marsupial cohorts. *Journal of Mammalian Evolution* **12**, 461–494 (2005).
112. Oliveira, E. V., Goin, F. J. & Candela, A. M. Un nuevo marsupial "pseudodiprotodonte" del Paleoceno Medio de Itaborai (Brasil). Consideraciones sobre el origen, radiación y heterocronía en los Paucituberculata. *Ameghiniana* **33**, 468 (1996).
113. Muirhead, J. & Filan, S. *Yarala burchfieldi* (Peramelemorphia) from Oligo-Miocene deposits of Riversleigh, northwestern Queensland. *Journal of Paleontology* **59**, 127–134 (1995).
114. Tedford, R. H. & Kemp, N. R. Oligocene marsupials of the Geilston Bay local fauna, Tasmania. *American Museum Novitates* **3244**, 1–22 (1998).
115. Muirhead, J. & Archer, M. *Nimbacinus dicksoni*, a plesiomorphic thylacine (Marsupialia, Thylacinidae) from Tertiary deposits of Queensland and the Northern Territory. *Memoirs of the Queensland Museum* **28**, 203–221 (1990).
116. Archer, M., Godthelp, H., Gott, M., Wang, Y. & Musser, A. The evolutionary history of notoryctids, yingabalanarids, yalkaparidontids and other enigmatic groups of Australian mammals. *Australian Mammalogy* **21**, 13–15 (1999).
117. Wain, H. M., Lush, M., Ducluzeau, F. & Povey, S. Genew: the human gene nomenclature database. *Nucleic Acids Research* **30**, 169–171 (2002).

Supplementary figures

Supplementary Figure 1 | A dated species-level phylogeny of virtually all extant mammals obtained using supertree construction. The three trees are topologically identical and differ only in the inferred divergence times: a) best estimate of divergence times, b) lower 95% confidence interval dates, and c) upper 95% confidence interval dates.

See file Bininda_SupplData1.txt

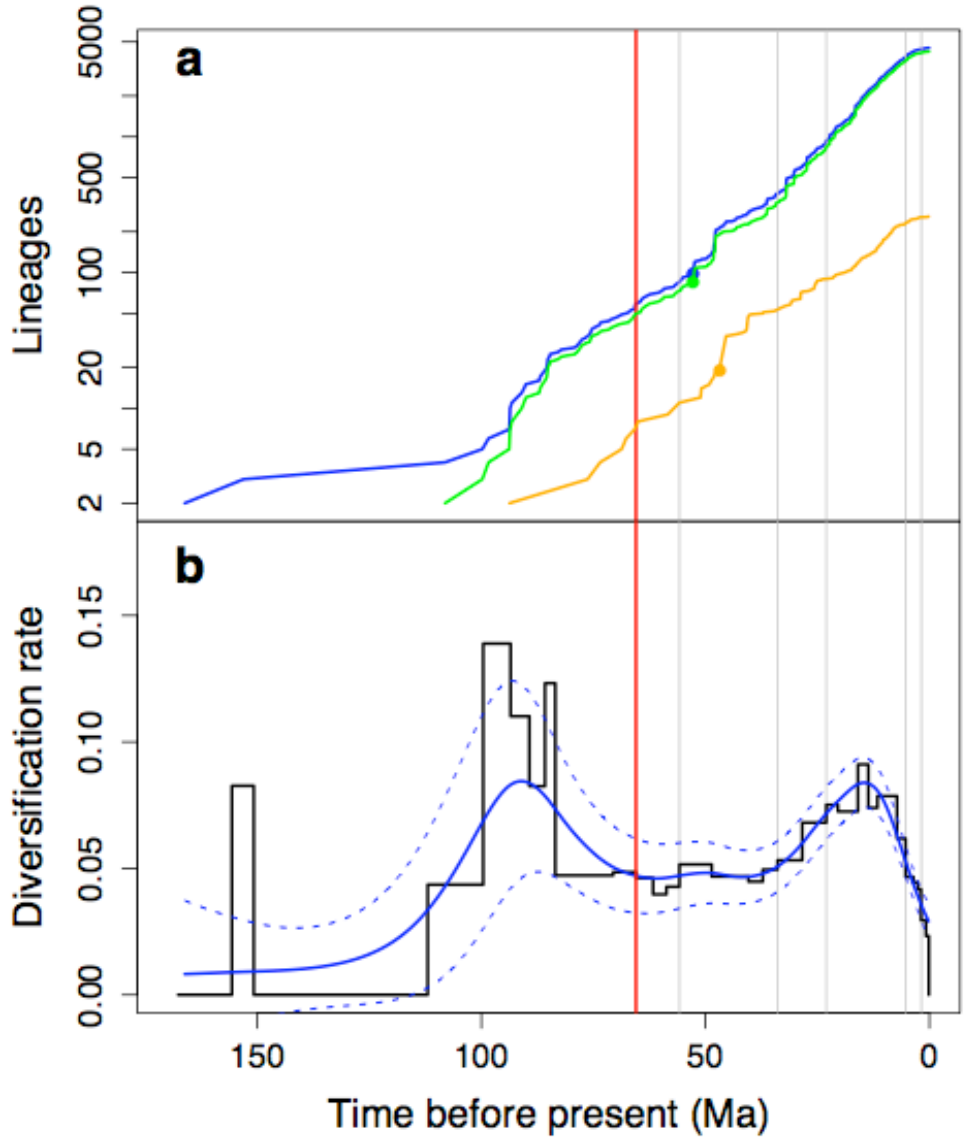

Supplementary Figure 2 | Temporal patterns of mammalian diversification based on upper confidence interval dates. a) Lineages-through-time plots showing diversification in all mammals (blue line), placental mammals only (green line), and marsupials only (orange line). Filled circles indicate when the degree of resolution in the phylogeny dropped below 85%; the associated analyses were restricted to the left of these points. The red vertical line is the K-T boundary; grey lines mark the boundaries between the Cenozoic epochs. b) Net rate of diversification through time. The stepped line shows diversification rate in each geological age or subepoch. The thick blue line shows the net mammalian diversification rate inferred from a generalised additive model of rate against time.

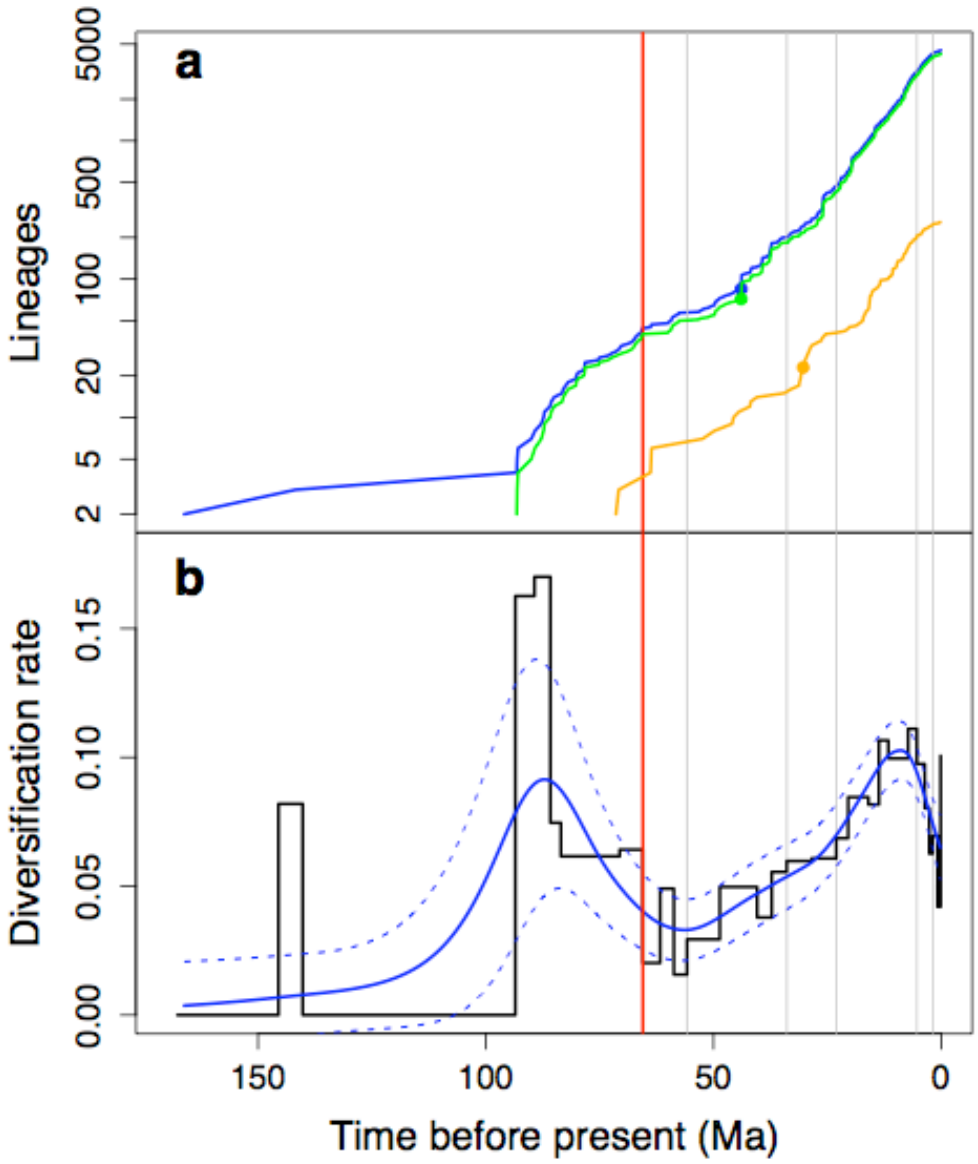

Supplementary Figure 3 | Temporal patterns of mammalian diversification based on lower confidence interval dates. a) Lineages-through-time plots showing diversification in all mammals (blue line), placental mammals only (green line), and marsupials only (orange line). Filled circles indicate when the degree of resolution in the phylogeny dropped below 85%; the associated analyses were restricted to the left of these points. The red vertical line is the K-T boundary; grey lines mark the boundaries between the Cenozoic epochs. b) Net rate of diversification through time. The stepped line shows diversification rate in each geological age or subepoch. The thick blue line shows the net mammalian diversification rate inferred from a generalised additive model of rate against time.

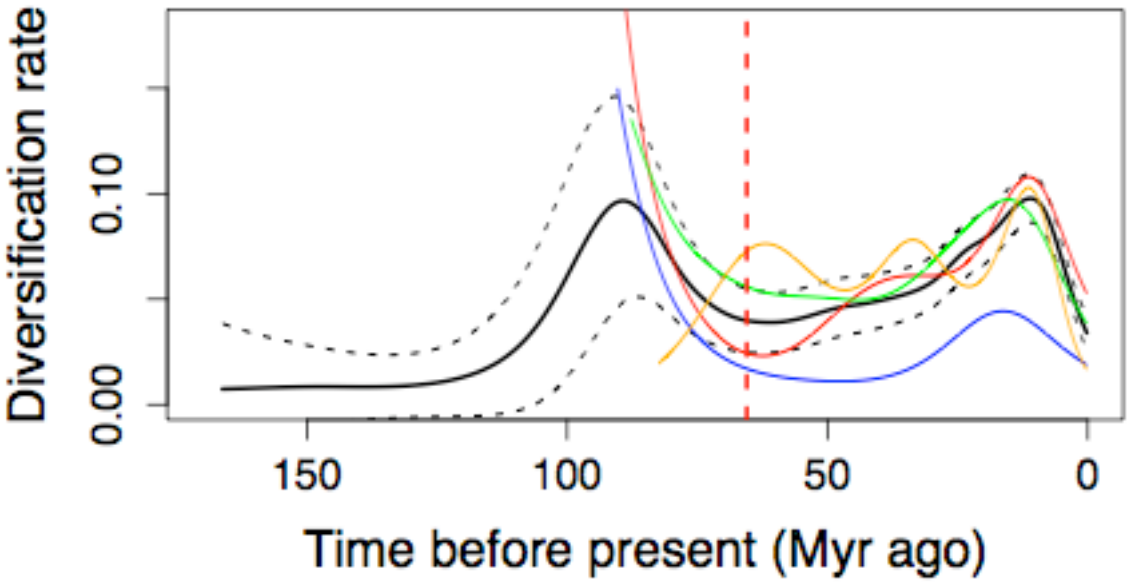

Supplementary Figure 4 | Net rates of diversification through time for selected mammalian lineages as inferred from a generalised additive model of rate against time. The lineages are Marsupialia (orange), combined Xenarthra/Afrotheria (blue), Laurasiatheria (green) and Euarchontoglires (red). The black line represents mammals as a whole (with dashed black lines indicating 95% confidence intervals).

Supplementary tables

Supplementary Table 1 | Statistics relating to the mammal supertree and component portions thereof, including references

Supertree	Number of taxa in tree	Number of extant taxa in Wilson and Reeder[23]	Percent completeness	Number of source trees	Number of characters	Resolution	Source
Afrosoricida	33	42	78.6	6	41	0.419	Grenyer and Purvis[90]
Carnivora	268	268	100.0	274	1304	0.782	Bininda-Emonds *et al.*[69]
Cetartiodactyla	290	290	100.0	198	2064	0.601	Price *et al.*[91]
Chiroptera	915	916	99.9	105	1858	0.469	Jones *et al.*[92]
Dermoptera	2	2	100.0	n/a	n/a	n/a	This study
Eulipotyphla	360	381	94.5	36	259	0.279	Grenyer and Purvis[90]; this study
Higher levels	113	113	100.0	725	6715	0.952	Beck *et al.*[49]
Hyracoidea	6	6	100.0	4	13	0.750	This study
Lagomorpha	79	79	100.0	149	672	0.974	Stoner *et al.*[93]
Macroscelidea	15	15	100.0	6	62	0.846	This study
Marsupialia	258	262	98.5	158	1775	0.742	Cardillo *et al.*[94]
Monotremata	3	3	100.0	n/a	n/a	1.000	This study
Perissodactyla	17	17	100.0	23	106	0.733	Price and Bininda-Emonds (in prep)
Pholidota	7	7	100.0	1	4	0.600	This study
Primates	233	233	100.0	298	2239	0.732	This study (data from refs 34,68)
Proboscidea	2	2	100.0	n/a	n/a	n/a	This study
Rodentia							
Anomaluridae	7	7	100.0	1	n/a	0.600	This study
Aplodontidae	1	1	100.0	n/a	n/a	n/a	This study
Castoridae	2	2	100.0	n/a	n/a	n/a	This study
Dipodidae	51	51	100.0	6	16	0.245	This study

doi: 10.1038/nature05634

Geomyoidea	91	94	96.8	54	405	0.652	Wong and Mooers (unpubl. data)
Hystricognathi	215	219	98.2	53	394	0.268	This study
Muridae	1304	1304	100.0	77	1920	0.239	This study
Myoxidae	26	26	100.0	16	110	0.500	This study
Pedetidae	1	1	100.0	n/a	n/a	n/a	This study
Sciuridae	271	273	99.3	35	366	0.717	This study
Scandentia	19	19	100.0	9	62	0.294	This study
Sirenia	4	4	100.0	2	4	1.000	This study
Tubulidentata	1	1	100.0	n/a	n/a	n/a	This study
Xenarthra	29	29	100.0	11	72	0.692	This study
Total / average	4510	4554	99.0	2622	20431	0.629	
Full tree	4510	4554	99.0	n/a	n/a	0.467	This study

Supertrees for taxa in italics were derived from a set of nested supertree analyses. In such cases, the number of source trees listed might be an overestimate given that a single source tree might have contributed to more than one analysis. The values for the Beck *et al.*[49] supertree refer to the full supertree as published, although it was collapsed to 65 taxa in deriving the full mammal supertree.

doi: 10.1038/nature05634

Supplementary Table 2 | Divergence time estimates for all nodes in the mammalian supertree.

Inferred ('best') dates are those obtained from the combination of relative molecular date estimates and fossil calibration points. Upper and lower bounds on these dates were obtained by multiplying the SE by 1.96 to derive the 95% confidence interval. For each of the sets of best, upper, and lower date estimates, divergence times were interpolated for all nodes missing inferred dates and all dates were corrected for negative branch lengths to derive the final date estimates.

See file Bininda_SupplData2.xls.

Supplementary Table 3 | Fossils used to calibrate local molecular clocks and establish divergence times.

Clade	Node number	Fossil age (Myr ago)	Fossil	Reference
Mammalia (root)	1	166.2	*Ambondro mahabo*	Flynn *et al.*[35]
Monotremata	2	63.6	*Monotrematum sudamericanum*	Pascual *et al.*[95]
Theria (Marsupialia + Eutheria)	4	127.5	*Eomaia scansoria*	Ji *et al.*[96]
Rodentia	10	57.25	*Tribosphenomys minutus*	Meng *et al.*[97]
Lagomorpha (Leporidae)	673	44.5	*Mytonolagus petersoni*	McKenna & Bell[42]
Scandentia	749	44.5	*Eodendrogale parvum*	Tong[98]
Dermoptera	750	37.15	*Dendrotherium major*	Ducrocq *et al.*[99]
Tarsiidae	752	44.5	*Tarsius eocaenus*	Beard *et al.*[100]
Suiformes (Artiodactyla)	933	52.2	*Diacodexis* sp.	Theodor *et al.*[101]
Cetacea	1051	52.2	*Pakicetus inachus*	Gingerich & Russell[102]
Perissodactyla	1106	52.2	*Orientolophis* sp.	Hooker[103]
Pholidota	1118	44.5	*Eomanis waldi*	Storch[104]
Canidae	1120	43.35	*Procynodictis vulpiceps*	McKenna & Bell[42]
Ursidae	1121	19.5	*Ursavus brevirhinus*	McKenna & Bell[42]
Phocidae	1182	19.5	*Pinnarctidion bishopi*	Wyss & Flynn[105]
Felidae + Hyaenidae	1238	31.15	*Proailurus jordani*	Hunt & Tedford[106]
Herpestidae + Viverridae	1275	25.72	*Palaeoprionodon lamandini*	Hunt & Tedford[106]
Chiroptera	1332	52.2	*Ageina tobieni*	Simmons[107]
Xenarthra (Dasypodidae)	1858	60.2	*Riostegotherium* sp.	Rose *et al.*[103]
Tubulidentata (Orycteropidae)	1878	19.5	*Myorycteropus africanus*	MacPhee[108]
Macroscelidea (Macroscelididae)	1879	37.15	*Metoldobotes stromeri*	McKenna & Bell[42]
Afrosoricida (Chrysochloridae)	1880	19.5	*Prochrysochloris miocaenicus*	MacPhee and Novacek[109]
Hyracoidea (Procaviidae)	1909	19.5	*Prohyrax* sp.	McKenna & Bell[42]
Sirenia (Trichechidae)	1910	13.79	*Potamosiren magdalensis*	McKenna & Bell[42]
Proboscidea (Elephantidae)	1917	19.5	*Stegalophodon nasaiensis*	Tassy *et al.*[110]
Didelphimorphia	1918	82.55	*Nortedelphys intermedius/magnus/minutus*	Case *et al.*[111]
Paucituberculata	1919	57.25	Unnamed paucituberculate	Oliveira *et al.*[112]
Peramelemorphia	1920	25.72	*Yarala burchfieldi*	Muirhead & Filan[113]
Diprotodontia	1945	25.72	Burramyidae indet.	Tedford & Kemp[114]
Dasyuromorphia	2013	19.5	*Nimbacinus dicksoni*	Muirhead and Archer[115]
Notoryctemorphia	2013	19.5	Unnamed notoryctid	Archer *et al.*[116]

doi: 10.1038/nature05634

References are to first describers if the placement of the target taxon is discussed in robust phylogenetic context; otherwise, references are to more recent authorities whose interpretations regarding ‘earliest’ clade representatives were followed in the analyses.

doi: 10.1038/nature05634

Supplementary Table 4 | Statistics relating to the 68 sequence data sets used for molecular dating, including the optimal model of evolution determined using ModelTEST[65] as automated using the Perl script autoMT v.1.0.

Gene	Genome	Number of taxa	Alignment length	Optimal model of evolution	LnL (nonclock)	ln L (clock)	LRT χ^2	LRT *P*-value
ADORA3	nDNA	78	336	TrN+I+G	6898.3042	7035.6425	274.68	2.81×10^{-24} *
ADRA2B	nDNA	63	1539	TVM+I+G	21561.5469	21779.2198	435.35	0 *
ADRB2	nDNA	80	1263	TVM+I+G	11986.3555	12144.99395	317.28	1.31×10^{-30} *
APOB	nDNA	76	1350	GTR+I+G	28412.4609	28733.64533	642.37	0 *
APP	nDNA	70	810	GTR+G	8227.2441	8335.87736	217.27	1.67×10^{-17} *
ATP7A	nDNA	74	690	TIM+I+G	11331.4033	11536.23304	409.66	0 *
BDNF	nDNA	98	804	K81uf+I+G	8092.7871	8345.11763	504.66	0 *
BMI1	nDNA	64	345	GTR+G	2423.5852	2503.45558	159.74	1.45×10^{-10} *
BRCA1	nDNA	149	3130	TVM+I+G	109566.1953	111450.9693	3769.5	0 *
CCR5	nDNA	151	1065	GTR+I+G	6934.5703	7095.21477	321.29	1.51×10^{-14} *
C-MOS	nDNA	69	489	HKY+I+G	3304.0105	3361.83578	115.65	0.0002079 *
C-MYC (1)	nDNA	41	582	K81uf+I+G	4459.5967	4523.68583	128.18	1.96×10^{-11} *
C-MYC (2)	nDNA	48	850	TVM+I+G	5717.2114	6085.16562	735.91	0 *
CNR1	nDNA	93	1101	TVM+I+G	14831.8223	15038.93738	414.23	0 *
CREM	nDNA	72	476	TVM+I+G	6758.9014	7108.57896	699.36	0 *
EDG1	nDNA	69	978	TVM+I+G	11895.6943	12170.46151	549.53	0 *
GHR	nDNA	148	2127	TVM+I+G	36693.5703	37549.16591	1711.2	7.56×10^{-234} *
K-CASEIN	nDNA	58	651	K81uf+G	5120.7769	5233.68563	225.82	2.94×10^{-22} *
LCAT (1)	nDNA	44	540	TIM+I+G	5647.9297	5734.96337	174.07	5.25×10^{-18} *
LCAT (2)	nDNA	33	677	K81uf+I+G	4759.6548	6233.43173	2947.6	0 *
MC1R	nDNA	102	1050	GTR+I+G	10465.8291	10587.74169	243.83	5.07×10^{-14} *
MT-ATP6	mtDNA	202	711	GTR+I+G	39820.1211	40323.73938	1007.2	2.03×10^{-102} *
MT-ATP8	mtDNA	190	213	GTR+I+G	12864.0479	13157.98091	587.87	1.01×10^{-41} *
MT-CO1	mtDNA	223	1572	GTR+I+G	84044.3281	84786.8918	1485.1	6.86×10^{-173} *
MT-CO2	mtDNA	415	711	GTR+I+G	58943.0938	60165.7638	2445.3	3.30×10^{-267} *
MT-CO3	mtDNA	283	858	GTR+I+G	50890.4258	51708.44874	1636	3.28×10^{-178} *

doi: 10.1038/nature05634

MT-CYB	mtDNA	1284	1203	GTR+I+G	Inf	414095.1784	n/a	n/a
MT-ND1	mtDNA	366	996	GTR+I+G	88077.79355	86000.3828	4154.8	0 *
MT-ND2	mtDNA	283	1068	GTR+I+G	101684.73	100571.9297	2225.6	4.85×10^{-274} *
MT-ND3	mtDNA	325	363	TVM+I+G	33808.2335	32856.8477	1902.8	4.96×10^{-208} *
MT-ND4	mtDNA	324	1467	GTR+I+G	115930.2765	114448.4531	2963.6	0 *
MT-ND4L	mtDNA	352	297	GTR+I+G	29594.63204	28910.6465	1368	6.78×10^{-116} *
MT-ND5	mtDNA	166	1869	GTR+I+G	109605.1155	108897.1562	1415.9	3.27×10^{-180} *
MT-ND6	mtDNA	154	561	GTR+I+G	30724.26384	30424.0059	600.52	1.12×10^{-52} *
MT-RNR1	mtDNA	810	1165	GTR+I+G	Inf	188550.8637	n/a	n/a
MT-RNR2	mtDNA	744	2702	GTR+I+G	Inf	334214.3762	n/a	n/a
MT-TA (tRNA-ALA)	tRNA	140	72	GTR+I+G	1977.76845	1843.5509	268.44	2.36×10^{-10} *
MT-TC (tRNA-CYS)	tRNA	140	79	K81uf+G	2299.60263	2180.4097	238.39	2.57×10^{-7} *
MT-TD (tRNA-ASP)	tRNA	115	76	GTR+G	2112.72495	2006.1035	213.24	4.15×10^{-8} *
MT-TE (tRNA-GLU)	tRNA	122	76	GTR+G	1983.40447	1880.9731	204.86	2.35×10^{-6} *
MT-TF (tRNA-PHE)	tRNA	201	86	TrN+I+G	3022.24698	2857.5278	329.44	1.81×10^{-8} *
MT-TG (tRNA-GLY)	tRNA	210	86	TrN+I+G	3132.40905	2977.1646	310.49	5.33×10^{-6} *
MT-TH (tRNA-HIS)	tRNA	276	74	TrN+I+G	3556.28727	3349.7217	413.13	1.11×10^{-7} *
MT-TI (tRNA-ILE)	tRNA	123	75	TIM+I+G	1123.53535	1049.6792	147.71	0.04978
MT-TK (tRNA-LYS)	tRNA	128	80	GTR+I+G	2524.863	2388.4656	272.79	1.00×10^{-12} *
MT-TM (tRNA-MET)	tRNA	129	75	GTR+I+G	790.67	708.9114	163.52	0.01605
MT-TN (tRNA-ASN)	tRNA	125	78	TrN+I+G	1851.27988	1725.6079	251.34	9.42×10^{-11} *
MT-TP (tRNA-PRO)	tRNA	319	125	TIM+I+G	3777.29426	3527.1602	500.27	2.33×10^{-10} *
MT-TQ (tRNA-GLN)	tRNA	119	79	HKY+I+G	2192.13453	2096.7307	190.81	2.01×10^{-5} *
MT-TR (tRNA-ARG)	tRNA	268	77	TVM+I+G	3506.82404	3305.2341	403.18	1.15×10^{-7} *
MT-TS1 (tRNA-SER)	tRNA	156	84	GTR+G	1811.0682	1701.1661	219.8	0.0004005 *
MT-TT (tRNA-THR)	tRNA	224	89	TrN+G	4119.64955	3905.2583	428.78	3.44×10^{-15} *
MT-TV (tRNA-VAL)	tRNA	650	106	GTR+I+G	Inf	9431.412846	n/a	n/a
MT-TW (tRNA-TRP)	tRNA	139	83	GTR+I+G	2362.75406	2214.3738	296.76	1.09×10^{-13} *
MT-TY (tRNA-TYR)	tRNA	139	73	TVM+G	1992.0419	1868.7208	246.64	3.05×10^{-8} *
PLCB4	nDNA	74	410	TIM+I+G	8304.03184	8090.1567	427.75	0 *
PNOC	nDNA	74	585	TVM+I+G	5854.76346	5754.7935	199.94	5.60×10^{-14} *

PRNP	nDNA	164	948	GTR+I+G	13173.5078	13604.85418	862.69	6.43×10^{-91} *
PROTAMINE P1	nDNA	71	546	GTR+G	2137.1113	2362.04764	449.87	0 *
RAG1	nDNA	49	3198	GTR+I+G	25725.3242	27028.42481	2606.2	0 *
RAG2	nDNA	221	1593	TVM+I+G	27598.8926	28058.28759	918.79	4.75×10^{-83} *
RBP3	nDNA	549	1305	GTR+I+G	80086.1406	82116.89541	4061.5	0 *
SRY	nDNA	218	231	TrN+I+G	2557.6758	2651.64152	187.93	0.9164
TSPY	nDNA	87	481	TVMef+G	2372.3823	2406.14671	67.529	0.9181
TYR	nDNA	78	426	TVMef+I+G	7303.0513	7411.28994	216.48	2.02×10^{-15} *
VWF	nDNA	190	1276	TVM+I+G	57106.4805	58025.55815	1838.2	3.40×10^{-241} *
ZFX	nDNA	54	1185	GTR+I+G	4021.7144	4197.45086	351.47	4.75×10^{-46} *
ZFY	nDNA	73	1185	GTR+I+G	6096.2603	6340.98674	489.45	0 *

"Inf" means that PAUP* could not determine the log-likelihood value. The applicability of enforcing a molecular clock was tested using a likelihood ratio test (LRT) with *df* = number of taxa – 2; an asterisk indicates rejection of the hypothesis at a nominal alpha of 0.05 using a χ^2 distribution (the four untestable genes were conservatively assumed not to evolve according to a clock). Each of the genes *C-MYC* and *LCAT* included separate non-overlapping portions, designated with (1) and (2). Gene names are standardized according to the Human Genome Nomenclature Committee names[117].

doi: 10.1038/nature05634

Supplementary Table 5 | Occurrence of mammalian genera in 11 geological periods (subepochs) from Late Triassic until Late Eocene using the Unitaxon database[42].

Upper, lower and mid-range times (in millions of years) of the geological periods followed[89]. Genera were split into one of two groups: (1) genera whose family diversity was exclusively or predominantly Paleocene or older (≥55.8Ma) and (2) genera whose family diversity was exclusively or predominantly Eocene or younger (<55.8Ma).

See file Bininda_SupplData3.xls.